



# Canadian Journal of Earth Sciences

## Nd isotope mapping of the Grenvillian Allochthon Boundary Thrust in Algonquin Park, Ontario

Journal:	<i>Canadian Journal of Earth Sciences</i>
Manuscript ID	cjes-2018-0142.R1
Manuscript Type:	Article
Date Submitted by the Author:	26-Sep-2018
Complete List of Authors:	Dickin, Alan; School of Geography and Geology Strong, Jacob; School of Geography and Geology
Keyword:	Nd isotopes, Model ages, Grenville Province
Is the invited manuscript for consideration in a Special Issue? :	Not applicable (regular submission)

SCHOLARONE™  
Manuscripts

1 **Nd isotope mapping of the Grenvillian Allochthon Boundary Thrust in Algonquin Park,**  
2 **Ontario**

3

4 A.P. Dickin and J.W.D. Strong

5 School of Geography and Earth Sciences, McMaster University, Hamilton ON, Canada

6

7 **Abstract**

8 Over fifty new Nd isotope analyses are presented for high-grade orthogneisses from  
9 Algonquin Park and surrounding region in order to map major Grenvillian thrust boundaries. Nd  
10 model ages display a consistent geographical pattern that allows detailed mapping of the  
11 boundary between the Algonquin and Muskoka domains, here interpreted as the local trajectory  
12 of the Ottawa-age Allochthon Boundary Thrust (ABT). The ABT is underlain by a domain with  
13 Paleoproterozoic Nd model ages, interpreted as a tectonic duplex entrained onto the base of the  
14 main allochthon. The boundaries determined using Nd isotope mapping are consistent with field  
15 mapping and with remotely sensed aeromagnetic and digital elevation data. The precise location  
16 of the ABT can be observed in a road-cut on Highway 60, on the north shore of the Lake of Two  
17 Rivers in the centre of Algonquin Park.

18

19 **Introduction**

20 Algonquin Park forms part of the Canadian Shield located in the Grenville Province of  
21 Ontario (Fig. 1). The Grenville Province represents the deeply exhumed remains of an ancient  
22 orogenic belt with similarities to the modern Himalayas. Like the Himalayas, the Grenville  
23 Province experienced crustal thickening due to a continental collision, and then underwent

24 gravitational collapse by thrusting. However, the exact locus of this thrusting has proven difficult  
25 to determine.

26 In their early work on this subject, Rivers et al. (1989) recognised the principal locus of  
27 Ottawa-age (1080 Ma) thrusting as a major shear zone separating a belt of relatively *in situ*  
28 crustal basement to the NW from a belt of laterally transported ‘allochthonous’ thrust sheets to  
29 the SE. This boundary, termed the Allochthon Boundary Thrust (ABT) was believed to follow  
30 round the north side of Parry Sound domain on Georgian Bay, before traversing eastward with a  
31 trajectory sub-parallel to the Monocyclic Belt Boundary (MBB, Fig.1).

32 This model was abandoned in later work (e.g. Rivers et al., 2002), and a more northerly  
33 trajectory was proposed, based on the discovery of allochthonous rocks near North Bay, Ontario  
34 (Ketchum and Davidson, 2000). However, it was shown in several subsequent papers (Dickin  
35 and McNutt, 2003; Dickin et al., 2012; 2014) that the allochthonous rocks at North Bay (NB,  
36 Fig. 1) represent a tectonic outlier or klippe. Hence, Dickin et al. (2017) reinstated the southerly  
37 trajectory for the ABT originally proposed by Rivers et al. (1989) in the Georgian Bay area.  
38 However, this work did not examine the trajectory of the ABT eastward into Algonquin Park,  
39 which is the focus of the present study.

40

## 41 **The Geology of Algonquin Park**

42 Based on its large size (7723 square km) and proximity to major population centres,  
43 Algonquin Park could form a public showcase of the geology of the Precambrian Shield.  
44 However, its geology has been difficult to unravel for a number of reasons. Some difficulties  
45 arise from limited vehicle access to the park interior and extensive glacial cover. However, the  
46 main difficulty is the high degree of crustal exhumation experienced by Grenvillian gneisses. As

47 a result, most of the rocks in Algonquin Park consist of high-grade granitoid orthogneisses with  
48 few distinguishing features. In fact, a geological overview of Algonquin Park has never been  
49 achieved.

50 In the beginning of modern geological mapping in the gneiss belt of Ontario, geological  
51 structures were mapped with the assistance of aerial photography, which vividly picked out the  
52 locations of major deformation zones in the Parry Sound region (Davidson et al., 1982; Culshaw  
53 et al., 1983). These deformation zones were interpreted as tectonic boundaries between distinct  
54 'lithotectonic' domains. This work established a series of distinct units, including the Parry  
55 Sound domain itself, and the Algonquin domain to the east (Fig. 2).

56 The Algonquin domain was separated from the Muskoka domain to the south by a major  
57 shear zone (solid black line, Fig. 2), and from the Kiosk domain to the north by another less-  
58 distinct shear zone (dotted black line). The Algonquin domain was also subdivided into a number  
59 of sub-domains (Culshaw et al., 1983), which were well established to the west of the park, but  
60 became less clearly defined within the park itself. Around the same time, Lumbers (1982),  
61 working on the eastern side of Algonquin Park, coined the term 'Algonquin Batholith' to signify  
62 the igneous protolith of rocks in this area. However, these rocks do not form a batholith in the  
63 conventional sense, and the term is therefore not helpful.

64 During the 1990s, the main research focus continued to be in the Parry Sound area to the  
65 west. Here, the GLIMPCE and Lithoprobe seismic reflection profiles supported the structural  
66 model of this region as a stack of thrust slices (Culshaw et al., 1983; Culshaw et al., 1997).  
67 However, the geology of Algonquin Park was largely neglected during this period.

68 A significant discovery made by Ketchum and Davidson (2000), following earlier work  
69 by Davidson and Grant (1986) and Culshaw et al. (1994), was that different levels in the thrust

70 stack could be distinguished by the presence of different metabasic intrusive bodies. Specifically,  
71 the lowest structural level (Britt domain of Davidson, 1984) contained metamorphosed  
72 equivalents of 1240 Ma Sudbury diabase dykes, whereas higher structural levels (including  
73 Algonquin and Muskoka domains) contained ca. 1160 Ma coronitic olivine metagabbro (black  
74 stars in Fig. 2). The latter two structural decks were therefore argued to be allochthonous relative  
75 to the underlying Britt parautochthon.

76 Ketchum and Davidson (2000) joined the most northwesterly outcrops of the  
77 allochthonous units to redefine the trend of the ABT (green dashed line passing through North  
78 Bay in Fig. 2). This trajectory was much further north than originally proposed by Rivers et al.  
79 (1989), and now included all of Algonquin Park within the allochthon. This proposal was  
80 described by the original authors as a speculative model, but was adopted by most subsequent  
81 workers, beginning with Rivers et al. (2002). However, there was little scientific basis for this  
82 interpretation of Algonquin Park, since the region along the northern edge of the park (including  
83 the Kiosk type-locality) contains very little meta-basic rock, and is therefore of equivocal affinity  
84 in this model.

85 Since it is based on the presence of younger metabasic rocks, the mapping approach of  
86 Ketchum and Davidson (2000) is a proxy method. It characterizes the crust on either side of the  
87 ABT boundary by one aspect of their different geological histories, rather than by actual field  
88 mapping of the boundary itself. Nd isotope mapping is another proxy approach to mapping the  
89 ABT, based on the observation that crust on either side of the boundary has distinct ranges of Nd  
90 model ages, reflecting different crustal formation ages (Dickin, 2000). However, unlike the  
91 sporadic distribution of metabasic rocks, Nd model ages can be determined on any granitoid

92 orthogneiss. This makes Nd isotope mapping a much more geographically precise method for  
93 mapping terrane boundaries such as the ABT.

94 Dickin and McNutt (2003) showed that in the North Bay area, where metabasic outcrops  
95 are numerous (Fig.2), Nd isotope mapping yields results fully consistent with the distribution of  
96 metabasic rocks. They concluded that allochthonous rocks in this area form a tectonic outlier or  
97 klippe (NB Fig 3), and are not attached to the main allochthon to the south.

98 Where metabasic rocks are sparse, such as the northern part of Algonquin Park, Nd  
99 isotope mapping offers the only effective method for distinguishing parautochthonous and  
100 allochthonous crustal affinities. Hence, Dickin et al. (2014) showed that all of the northern part  
101 of Algonquin Park consists of Paleoproterozoic parautochthonous crust, except for a small  
102 allochthonous klippe near Brent (to be discussed below).

103

#### 104 **The duplex model**

105 The area in Fig 1 marked by a question-mark corresponds to the Lac Dumoine thrust  
106 sheet, which is shown in Fig. 3 based on later geological mapping. The location of the ABT  
107 under this thrust sheet was first mapped in detail by Indares and Dunning (1997) at Lac Watson  
108 (LW, Fig. 3). However, these authors also showed that an additional structural deck was present  
109 in this region, between Archean basement (pink in Fig. 3) and the Mesoproterozoic allochthon  
110 (pale green). Nd isotope mapping of this structural deck by Herrell et al. (2006) revealed  
111 Paleoproterozoic Nd model ages (averaging 1.9 Ga). This work was extended by Dickin et al.  
112 (2012), who showed that this unit forms a nearly continuous band of Paleoproterozoic crust  
113 (yellow in Fig. 3) round the main Mesoproterozoic allochthon. Hence they proposed that this

114 deck represents a tectonic duplex entrained onto the base of the allochthon during NW-directed  
115 Ottawa-age thrusting.

116 In the Parry Sound region the crustal structure is more complex, since Parry Sound  
117 domain itself represents an additional structural deck overlying the main allochthon. Lithoprobe  
118 transects (White et al., 1994) showed that dense rock in Parry Sound domain caused loading of  
119 the crust in this area, down-buckling the underlying allochthon (see cross-section in Fig. 3).  
120 However, reinterpretation of Lithoprobe line 31 by Dickin et al. (2014; 2017) showed that the  
121 overall trajectory of the ABT has a ramp-flat style, with only local down-buckling under Parry  
122 Sound domain. This explains the appearance of parautochthonous Paleoproterozoic rocks at the  
123 surface in the Lower Rosseau domain (Fig. 3 cross section). Hence, the main ramp of the ABT is  
124 located under the Muskoka allochthon, southeast of the Lower Rosseau window (heavy dashed  
125 line in Fig. 3 cross-section).

126 Detailed Nd isotope mapping in the Parry Sound area (Dickin et al., 2017) showed that a  
127 tectonic duplex was also present under the main allochthon in this region (mauve in Fig. 3), but  
128 with somewhat younger Nd model ages (averaging ca. 1.7 Ga) than in the Quebec part of the  
129 duplex. However, the underlying Parautochthon is also younger in the Parry Sound area, since it  
130 corresponds to a Penokean arc that was accreted onto the Archean craton to the north (Dickin  
131 and McNutt, 1989). Hence, there appears to be a change in the age of *both* the parautochthon and  
132 the duplex across Algonquin Park, from 2.7 / 1.9 Ga in the Lac Dumoine region to 1.9 / 1.7 Ga in  
133 the Parry Sound region. This change is attributed to the derivation of crust in the Parry Sound  
134 region from a more outboard location in the pre-Grenvillian continental margin.

135 Detailed Nd isotope mapping in the Nobel area (Fig. 3 cross-section) showed that the  
136 boundary between late Paleoproterozoic (mauve) and Mesoproterozoic (green) crust corresponds

137 precisely to the ABT boundary mapped by Culshaw et al. (2004). This boundary (heavy dashed  
138 line in the cross section) is also the principal locus for pods of retrogressed eclogite, indicative  
139 of exhumation from the deep crust. This implies that the ABT in this area represents the  
140 horizontal extension of a crustal-scale ramp. However, an outcrop of coronitic olivine  
141 metagabbro (Heaman and LeCheminant, 1993) is found structurally *below* the ABT boundary in  
142 the Nobel area (Culshaw et al., 2004; Dickin et al., 2017). Hence, the boundary that separates  
143 rocks containing coronitic olivine metagabbro from rocks containing metamorphosed Sudbury  
144 diabase is not the ABT itself (as proposed by Ketchum and Davidson, 2000), but the sole thrust  
145 of the duplex. On the other hand, Nd model age distributions show that the eclogite-bearing ABT  
146 boundary below Parry Sound domain is equivalent to the basal shear zone of the Muskoka  
147 domain (Dickin et al., 2017). Hence, we are led back to the original conception of Davidson  
148 (1984) based on field mapping, that the sole thrust of the Muskoka domain is the major structural  
149 discontinuity of the gneiss belt, and is the local expression of the ABT.

150 As noted above, this was the model originally proposed by Rivers et al. (1989), but the  
151 trajectory of the Muskoka shear zone was unclear at its easterly end where it enters Algonquin  
152 Park (Fig. 2). The earliest proposed trajectory (solid black line, Culshaw et al., 1983) was  
153 approximately followed by Rivers and Schwerdtner (2015), shown by the pink dashed line. On  
154 the other hand, a more easterly trajectory proposed by Davidson (1984) was closely followed by  
155 Culshaw et al. (2016), shown by the orange dotted line in Fig. 2.

156 The area in the southerly part of Algonquin Park where these models differ is a very  
157 inaccessible area, but the alternative trajectories are separated by only a few km where they cross  
158 Highway 60 in Algonquin Park, which has an abundance of road cuts. This is an ideal opportunity  
159 to test these models using detailed Nd isotope mapping, and it offers the possibility of a road section  
160 displaying the ABT for easy viewing.

161

**162 Sampling and analytical techniques**

163 The objective of Nd isotope mapping is to characterize the protolith age (crustal  
164 formation age) of large areas of crust as an indication of the geological relationships between  
165 highly metamorphosed lithotectonic terranes. The protolith age is one of the most fundamental  
166 features of a crustal terrane, but clearly there are other events in the geological history of terranes  
167 that are also indicative of relationships between them.

168 Another feature that may characterise lithotectonic terranes and domains is their  
169 magmatic / plutonic history. In the SW Grenville Province, the most widely distributed igneous  
170 crystallisation event occurred around 1.45 Ga (Slagstad et al., 2004, 2009, and references  
171 therein). Rocks with U-Pb ages corresponding to this event are found in most of the lithotectonic  
172 domains shown in Fig. 3, except for the Monocyclic Belt in the SE corner. Some older U-Pb ages  
173 are also found in the northern part of the study area (Nadeau and van Breemen, 1998, and  
174 references therein). However, these U-Pb ages are much too thinly scattered to be used to map  
175 the complexly deformed terrane boundaries in this region. In contrast, Nd isotope analysis  
176 represents a cost-effective technique for mapping lithotectonic terranes, based on the robustness  
177 of Nd isotope signatures in highly metamorphosed terranes (e.g. Dickin, 2000). This method  
178 allows very high spatial resolution, which is unmatched by any other geological age discriminant  
179 in the Grenville Province.

180 Since the objective of this study was to characterize the protolith age of the crust as an  
181 estimate of its regional crustal formation age, sampling was limited to granitoid orthogneisses  
182 that are believed to form by anatexis of mafic juvenile arc crust. Previous studies have shown  
183 that granitoids of this type have Nd isotope signatures that are consistent and predictable (e.g.

184 McNutt and Dickin, 2012), thus allowing reliable estimates to be made of the formation age of  
185 the crust using the depleted mantle model of DePaolo (1981).

186 The lithologies of the analysed samples were determined by hand-lens examination. All  
187 of the sampled rocks are clearly orthogneissic, and their lithologies are summarised in Table 1  
188 using the Streckeisen classification. Gneisses in the range diorite – monzodiorite – quartz  
189 monzodiorite – granodiorite are dominant in the allochthon. On the other hand, the duplex is  
190 slightly more siliceous and alkaline, being dominated by monzogranite gneiss. The smaller  
191 sample set from the parautochthon is dominantly granodioritic. These lithologies are all typical  
192 of ensialic arc magmatism (Martin and Dickin, 2005).

193 In contrast to granitoid rocks, sampling of mafic gneisses was avoided as far as possible,  
194 because of the increased likelihood of a younger mantle-derived component in these rock-types.  
195 Metasedimentary gneisses were also excluded because of their uncertain sedimentary  
196 provenance. Most analysed samples contain amphibole, but feldspars are commonly green-  
197 coloured. Therefore, although the dominant metamorphic grade is upper amphibolite facies,  
198 many samples are probably retrogressed from granulite facies.

199 On average, 1 kg of rock was crushed, after the removal of weathered, veined or  
200 migmatized material, and careful attention was given to obtain a fine powder representative of  
201 the whole rock. Sm-Nd analysis followed our established procedures. After a four-day  
202 dissolution at 125°C using HF and HNO<sub>3</sub>, samples were converted to the chloride form before  
203 being split, and one aliquot spiked with a mixed <sup>150</sup>Nd-<sup>149</sup>Sm spike. Analysis by this technique  
204 yielded Sm/Nd = 0.2280 +/- 2 for BCR-1. Standard cation and reverse phase column separation  
205 methods were used. Nd isotope analyses were performed on a VG isomass 354 mass  
206 spectrometer at McMaster University using double filaments and a 4 collector peak switching

207 algorithm, and were normalised to a  $^{146}\text{Nd}/^{144}\text{Nd}$  ratio of 0.7219. Average within-run precision  
208 on the samples was  $\pm 0.000012$  ( $2\sigma$ ), and an average value of  $0.51185 \pm 2$  ( $2\sigma$  population) was  
209 determined for the La Jolla Nd standard. Because the work extended over several years, some  
210 samples were duplicated to check for long-term reproducibility of  $^{147}\text{Sm}/^{144}\text{Nd}$  and  $^{143}\text{Nd}/^{144}\text{Nd}$   
211 ratios, which are estimated at 0.1% and 0.002% ( $1\sigma$ ) respectively, leading to an analytical  
212 uncertainty on each model age of ca. 20 Ma ( $2\sigma$ ).

213

## 214 **Results**

215 New Nd data for over fifty samples from the Algonquin region are presented in Table 1,  
216 where they are used to calculate TDM ages using the depleted mantle model of DePaolo (1981).  
217 As discussed by Dickin et al. (2016), this model yields formation ages for crustal terranes in the  
218 SW Grenville Province that are very well supported by U-Pb dating (Slagstad et al., 2004; 2009;  
219 McNutt and Dickin, 2012), thus validating the accuracy of the model.

220 Samples are grouped in Table 1 according to the new structural domains proposed in this  
221 study, and are shown on a coloured map in Fig. 4, where new data points from Table 1 are  
222 numbered, whereas published data points are un-numbered (Dickin and McNutt 1990; Dickin et  
223 al., 2008; 2010; Slagstad et al., 2009; Moore and Dickin, 2011). The new data form three main  
224 age categories: 1.45 – 1.64 Ga in the Muskoka allochthon, 1.65 – 1.79 Ga in the Algonquin  
225 duplex and 1.8 – 1.99 Ga in small domains near Cache Lake, Oxtongue Lake and Heron Lake  
226 that are interpreted as tectonic slivers brought to the surface from the underlying parautochthon.  
227 In addition, a few samples within the allochthonous domain have younger TDM ages in the  
228 range 1.35 – 1.44 Ga.

229 The crustal structures shown in Fig. 4 will be discussed in detail below. However, it is  
230 first important to visualize the Nd isotope data on the Sm/Nd isochron diagram (Fig. 5), in order  
231 to see the isotopic distribution of points that define the three main age suites. These suites are  
232 compared in Fig. 5 with corresponding suites of published data, and with 1.75 and 1.45 Ga  
233 reference lines.

234 Starting with the youngest suite, we can see that the new data for the main allochthon  
235 (bright green squares) are fully coincident with published data for the Muskoka domain (Slagstad  
236 et al., 2009; Dickin et al. 2010; 2017), and with a 1.45 Ga reference line that corresponds with  
237 the oldest U-Pb ages from the Muskoka domain (Slagstad et al., 2004; 2009). On the other hand,  
238 the average TDM model age of this suite (1.56 Ga, Table 1) reflects minor incorporation of  
239 slightly older crustal material during ensialic arc magmatism to form this suite.

240 The oldest crustal suite, interpreted as tectonic slivers of the parautochthon (yellow  
241 circles) mostly fall with the range of published data for the Paleoproterozoic Barilia terrane  
242 (Dickin et al., 2008), which lie on a 1.75 Ga reference line. The average TDM age of the Barilia  
243 suite is 1.9 Ga, attributed to an accreted Penokean arc terrane (Dickin and McNutt, 1989). This  
244 age has been supported by U-Pb detrital zircon ages from the north-west part of Algonquin Park  
245 (Culshaw et al., 2016). However, intensive ensialic arc magmatism after arc accretion led to the  
246 1.75 Ga Sm-Nd isochron age for this suite, which is in agreement with the oldest U-Pb age of  
247 1.74 Ga for this terrane (Krogh et al., 1992). The new samples of the parautochthon fall slightly  
248 above the Barilia reference line, attributed to slightly greater degrees of Mesoproterozoic  
249 magmatic reworking in these samples, reflecting their more southerly location relative to the  
250 main body of parautochthonous rocks to the north (Fig. 4). The degree of divergence from the  
251 1.75 Ga reference line increases slightly as Sm/Nd falls. This is attributed to a preponderance of

252 more felsic lithologies in the younger magmatic reworking, consistent with ensialic arc  
253 magmatism.

254 The intermediate age-suite corresponds to the crustal domain interpreted as a tectonic  
255 duplex. This suite has TDM ages between the other two suites (average = 1.73 Ga), and also  
256 defines an intermediate slope on the isochron diagram. Given that the rocks of the parautochthon  
257 and the allochthon are attributed to an older continental margin that was telescoped by  
258 Grenvillian tectonism, younger TDM ages are attributed to rocks that once lay further outboard  
259 on this margin. Therefore, the rocks of the duplex are attributed to a crustal segment that was  
260 originally outboard of the accreted Penokean arc, but inboard of the 1.45 Ga continental margin  
261 arc (Dickin and McNutt, 1990; Slagstad et al., 2009). Given the average TDM age of 1.73 Ga, it  
262 is considered that this crustal segment was most likely formed in a late Paleoproterozoic  
263 continental margin arc. A small amount of available U-Pb data support this interpretation  
264 (Nadeau and van Breemen, 1998).

265 An alternative way of assessing the Nd isotope data is by calculating  $\epsilon$  Nd values at the  
266 average age of magmatic activity. The epsilon value can then be plotted against Nd concentration  
267 to evaluate petrogenetic/mixing models. It is important to calculate epsilon Nd at the same time  
268 for all samples, even if their crystallization ages differ, because we are looking for relative  
269 differences in the protolith composition (reflecting different crustal formation ages). The results  
270 in Fig. 6 show that the three age suites all have similar ranges of Nd content, but distinct epsilon  
271 Nd signatures consistent with different crustal extraction ages. The samples attributed to slices of  
272 parautochthonous crust fall within the upper part of the epsilon Nd envelope of Barilia, but with  
273 above-average Nd contents, consistent with being more magmatically reworked than *in situ*  
274 parautochthon to the north. This is consistent with the development of a 1.45 Ga ensialic arc on

275 an older margin consisting of crust with southward-younging crustal formation ages (as proposed  
276 above).

277

## 278 **Discussion**

279 The major objective of this study was to establish the location of the eastward extension  
280 of the Muskoka Shear Zone in Algonquin Park, argued above to represent the local expression of  
281 the ABT. Four different published trajectories for parts of this boundary are shown in Fig. 4, all  
282 of which extend eastward from the established boundary south of Huntsville (Nadeau, 1991;  
283 Nadeau and van Breemen, 1998). These will be compared with the boundary derived from  
284 isotope mapping, shown as a change in background colour from lilac to green.

285 The first 15 km eastward from the agreed section runs through Kawagama Lake, which  
286 therefore gives limited scope for detailed study of the boundary. Davidson (1984) and Rivers  
287 and Schwerdtner (2015) preferred a more southerly trajectory, whereas Lumbers and Vertolli  
288 (2003) and Culshaw et al. (2016) preferred a slightly more northerly one. The boundary of  
289 Lumbers and Vertolli (2003) seems to be based on more detailed geological mapping, and is  
290 supported by the isotope data (Fig. 4, sample #2).

291 To the east of the Lumbers and Vertolli map, the trajectories of Culshaw et al. (1983) and  
292 Rivers and Schwerdtner (2015) are in close agreement, whereas the boundary of Culshaw et al.  
293 (2016) deviates strongly to the east, following Davidson (1984). These trajectories come closer  
294 together as they approach Highway 60, where we have very detailed coverage of the boundary.  
295 Relative to our new data, the misfit with Rivers and Schwerdtner (2015) is a little over 1 km,  
296 which is double the thickness of the boundary-line on their regional-scale map. Hence, the  
297 agreement is almost within cartographical error on the road, but our boundary diverges strongly

298 from Rivers and Schwerdtner (2015) to the north of the highway. On the other hand, the original  
299 boundary of Culshaw et al. (1983) does not reach the highway, since their map stopped at 78.5  
300 degrees longitude, which happens to be 2.5 km west of our boundary section on Highway 60.

301 Due to the difficulties of sampling away from Highway 60, it is necessary to use remotely  
302 sensed data to extrapolate the ABT boundary across country to the north and south. This is done  
303 in Fig. 7, which shows a close-up view of the sample localities and boundaries from Fig. 4 in the  
304 central area of Algonquin Park. The background was made by draping the first vertical derivative  
305 of the total magnetic field from Culshaw et al. (2016) over a shaded digital elevation model  
306 (DEM) map from the Government of Ontario. The new ABT trajectory (black dashed line)  
307 departs from that of Schwerdtner and Rivers (2015) around 45.5° N, and displays a ca. 90° bend  
308 in the vicinity of the Lake of Two Rivers (near sample #35, Fig. 7). Our trajectory is consistent  
309 with the structural grain from the aeromagnetic and DEM data, whereas the approximately N—S  
310 trajectory of Schwerdtner and Rivers (2015) cuts across the structural grain. The trajectory of  
311 Culshaw et al. (2016) is consistent with the structural grain, but is located too far east. Our  
312 proposed basement sliver in the vicinity of Cache Lake is also consistent with the structural grain  
313 (black dotted line).

314 To pinpoint the exact location of the boundary on Highway 60, it is shown on a  
315 composite photograph of the outcrop in Fig. 8. Samples that yield ages typical of the allochthon  
316 and the duplex are located about 35 m apart, on either side of a boundary dipping at ca. 15° E.  
317 The footwall of the boundary shows relatively fine-scale tectonic banding, including what appear  
318 to be calcareous-rich horizons a few decimeters thick. This could possibly represent a true  
319 supracrustal sequence dominated by meta-volcanics, with intervening volcanoclastic sediments.

320 In contrast, the layering structurally above the boundary is much more massive, with  
321 orthogneissic rock units typically 2 – 3 meters thick.

322 Immediately above the boundary, the outcrop contains a lozenge of rock which causes  
323 some deviation of foliations in the overlying units. However, the thinly foliated units underlying  
324 thrust boundary hardly deviate, except in a tight fold around the leading edge of the lozenge (Fig.  
325 8). Hence it appears that this second-order structure has not significantly affected the main shear  
326 zone, which carried the main allochthon over the underlying Algonquin duplex.

327 Examination of road sections through the whole E—W section of Highway 60 shows that  
328 the rocks have very consistent dip. This can be confirmed by examination of rock-cuts on Google  
329 *Streetview*. The dip is consistently about 15 – 20 degrees east through most of the park, before  
330 the road turns southwards at its eastern end towards Whitney. This supports the claim of Rivers  
331 and Schwerdtner (2015) that the allochthon in this area is a synform. Rivers and Schwerdtner  
332 (2015) named this NW-directed nappe the Wallace domain. However, this seems an  
333 unsatisfactory name, since the (very small) hamlet of Wallace is actually located far from the  
334 relatively well-defined synformal thrust sheet in the southerly part of Algonquin Park. Therefore,  
335 we consider it more appropriate to refer to this nappe as the Opeongo domain, as proposed by  
336 (Culshaw et al., 2016). Although those authors did not define an easterly limit to this domain,  
337 their foliation measurements (from within the limits of our proposed domain) demonstrate that it  
338 has a synformal structure typical of a nappe.

339 In view of the consistent eastward dip along most of Highway 60, the repetition of three  
340 slivers of parautochthonous crust seems slightly problematical. However, we suggest that this  
341 pattern can be explained by imbrication of the tectonic duplex in this area, which is not  
342 surprising for such a rock package. For example, it was proposed by Dickin et al. (2017) that the

343 Algonquin duplex is a relatively thin structural unit, whose large outcrop area is a coincidence  
344 due to the horizontal structural dip of the allochthon in this area. However, in that case, it seems  
345 very likely that additional slivers of parautochthonous crust are present elsewhere, and also  
346 possibly additional klippen of the allochthon overlying it. However, mapping these structures  
347 away from the highway will be difficult.

348 A final brief discussion should be made of the lower boundary of the Algonquin duplex  
349 against parautochthonous crust to the north. Fig. 2 shows a large group of metabasic outcrops in  
350 the northern central part of Algonquin Park (Davidson and Grant, 1986). These metabasic rocks  
351 were identified by Ketchum and Davidson (2000) as coronitic olivine metagabbros indicative of  
352 the allochthon. To test this affinity, we sampled two localities (# 42 and 43) near the NE end of  
353 the area of metagabbro outcrops. The TDM ages, and especially the  $\epsilon$  Nd (1.5 Ga) values, are  
354 typical of the Algonquin domain. Hence, we identify this area as part of the Algonquin duplex.  
355 In Fig. 4, we have shown this area connected to the main body of Algonquin domain as a NE-  
356 trending salient. However, it is also possible that this represents a tectonic outlier that is  
357 disconnected from the main body of Algonquin domain.

358 At the northern edge of the park, an area of rocks with Mesoproterozoic TDM ages  
359 typical of the allochthon was observed near Brent (Fig. 4). This is an area with good access, and  
360 detailed sampling allowed us to show that the Brent domain is an allochthonous klippe (Dickin et  
361 al., 2014). Unfortunately, the concentration of metabasic outcrops is in a more inaccessible area,  
362 and we have not yet been able to sample this region.

363

## 364 **Conclusions**

365 We conclude that the original field mapping of Culshaw et al. (1983) is the most  
366 consistent with our Nd isotope data. The structural interpretation of Culshaw et al. (1983) was  
367 largely followed by Davidson (1984) and Rivers et al. (1989), but was abandoned by Ketchum  
368 and Davidson (2000), Rivers et al. (2002) and Culshaw et al. (2016). However, tectonic mapping  
369 in deeply exhumed gneiss terranes can be somewhat subjective, since it may not be clear which  
370 of the observed shear zones is most significant. Hence, we conclude that terrane mapping in the  
371 Grenville Province needs to be tested and validated with Nd isotope data in order to reach  
372 reliable conclusions. In the present case, the original field mapping, not influenced by a  
373 preconceived structural model, was apparently the most perceptive. Based on the new isotope  
374 data and a re-examination of the highway section, we propose that the ABT, representing the  
375 principle thrust of the Ottawa orogeny, cuts across the Lake of Two Rivers with an  
376 approximately N—S trajectory, and is well exposed on Highway 60 with a 15° E dip.

377

### 378 **Acknowledgments**

379 We are grateful to the Ontario Ministry of Natural Resources and Forestry for permission to  
380 sample in Algonquin Park, and we thank Alison Lake and her staff for arranging access and  
381 sampling permits. APD thanks Tom Nagy for assistance in the field, and JWDS thanks  
382 McMaster University for scholarship support. We acknowledge constructive comments from the  
383 journal editor and reviewers that helped improve this paper.

384

### 385 **References**

- 386 Culshaw, N.G., Corrigan, D., Ketchum, J.W.F., Wallace, P. and Wodicka, N. 2004. Precambrian  
387 geology, Naiscoot area. Ontario Geological Survey. Preliminary map P.3549, scale  
388 1:50000.
- 389 Culshaw, N., Davidson, A. and Nadeau, L., 1983. Structural subdivisions of the Grenville  
390 province in the Parry Sound-Algonquin region, Ontario. Current Research, Part B,  
391 Geological Survey of Canada, Paper 83-1B, 243-252.
- 392 Culshaw, N., Foster, J., Marsh, J., Slagstad, T. and Gerbi, C., 2016. Kiosk domain, Central  
393 Gneiss Belt, Grenville Province, Ontario: A Labradorian palimpsest preserved in the  
394 ductile deep crust. *Precambrian Research* 280, 249-278.
- 395 Culshaw, N.G., Jamieson, R.A., Ketchum, J.W.F., Wodicka, N., Corrigan, D. and Reynolds, P.H.  
396 1997. Transect across the northwestern Grenville orogen, Georgian Bay, Ontario:  
397 Polystage convergence and extension in the lower orogenic crust: *Tectonics* 16, 966-982.
- 398 Culshaw, N.G., Ketchum, J.W.F., Wodicka, N. and Wallace, P. 1994. Deep crustal ductile  
399 extension following thrusting in the southwestern Grenville Province, Ontario. *Canadian*  
400 *Journal of Earth Sciences* 31, 160-175.
- 401 Davidson, A., 1984. Tectonic boundaries within the Grenville Province of the Canadian Shield.  
402 *Journal of Geodynamics*, 1, 433-444.
- 403 Davidson, A., Culshaw, N. and Nadeau, L., 1982. A tectono-metamorphic framework for part of  
404 the Grenville Province, Parry Sound region, Ontario. Current Research, Part A,  
405 Geological Survey of Canada, Paper 82-1A, 175-190.
- 406 Davidson, A. and Grant, S.M., 1986. Reconnaissance geology of western and central Algonquin  
407 Park and detailed study of coronitic olivine metagabbro, Central Gneiss Belt, Grenville

- 408 Province of Ontario. Current research, Part B, Geological Survey of Canada, Paper 86-  
409 1B, 837-848.
- 410 DePaolo, D.J. 1981. Neodymium isotopes in the Colorado Front Range and crust-mantle  
411 evolution in the Proterozoic. *Nature* 291, 193-196.
- 412 Dickin, A.P. 2000. Crustal formation in the Grenville Province: Nd-isotope evidence. *Canadian*  
413 *Journal of Earth Sciences* 37, 165-181.
- 414 Dickin, A.P., Cooper, D., Guo, A., Hutton, C., Martin, C., Sharma, K.N.M. and Zelek, M. 2012.  
415 Nd isotope mapping of the Lac Dumoine thrust sheet: implications for large scale crustal  
416 structure in the SW Grenville Province. *Terra Nova* 24, 363-372.
- 417 Dickin, A.P., Herrell, M., Moore, E., Cooper, D. and Pearson, S. 2014. Nd isotope mapping of  
418 allochthonous Grenvillian klippen: evidence for widespread 'ramp-flat' thrust geometry  
419 in the SW Grenville Province. *Precambrian Research* 246, 268-280.
- 420 Dickin, A., Hynes, E., Strong, J. and Wisborg, M. 2016. Testing a back-arc 'aulacogen' model for  
421 the Central Metasedimentary Belt of the Grenville Province. *Geological Magazine*, 153,  
422 681-695.
- 423 Dickin A.P. and McNutt, R.H. 1989. Nd model age mapping of the southeast margin of the  
424 Archean foreland in the Grenville province of Ontario. *Geology* 17, 299-302.
- 425 Dickin, A.P. and McNutt, R.H. 1990. Nd model-age mapping of Grenville lithotectonic domains:  
426 Mid-Proterozoic crustal evolution in Ontario, In: Gower, C.F., Rivers, T. and Ryan, B.,  
427 eds., *Mid-Proterozoic Laurentia–Baltica: Geological Association of Canada Special*  
428 *Paper* 38, 79-94.

- 429 Dickin, A.P. and McNutt, R.H. 2003. An application of Nd isotope mapping in structural  
430 geology: delineating an allochthonous Grenvillian terrane at North Bay, Ontario.  
431 Geological Magazine, 140, 539-548.
- 432 Dickin, A.P., McNutt, R.H., Martin, C. & Guo, A. 2010. The extent of juvenile crust in the  
433 Grenville Province: Nd isotope evidence. Geological Society of America Bulletin, 122,  
434 870-883.
- 435 Dickin, A.P., Moretton, K. and North, R. 2008. Isotopic mapping of the Allochthon Boundary  
436 Thrust in the Grenville Province of Ontario, Canada. Precambrian Research 167, 260-  
437 266.
- 438 Dickin, A., Strong, J., Arcuri, G., Van Kessel, A. and Krivankova-Smal, L., 2017. A revised  
439 model for the crustal structure of the SW Grenville Province, Ontario, Canada.  
440 Geological Magazine, 154, 903-913.
- 441 Heaman, L.M. and LeCheminant, A.N. 1993. Paragenesis and U-Pb systematics of baddeleyite  
442 (ZrO<sub>2</sub>). Chemical Geology 110, 95-126.
- 443 Herrell, M.K., Dickin, A.P. and Morris, W.A. 2006. A test of detailed Nd isotope mapping in the  
444 Grenville Province: delineating a duplex thrust sheet in the Kipawa Mattawa region.  
445 Canadian Journal of Earth Sciences 43, 421-432.
- 446 Indares A. and Dunning, G. 1997. Coronitic metagabbro and eclogite from the Grenville  
447 Province of western Quebec: interpretation of U-Pb geochronology and metamorphism:  
448 Canadian Journal of Earth Sciences 34, 891-901.
- 449 Ketchum, J.W.F. and Davidson, A. 2000. Crustal architecture and tectonic assembly of the  
450 Central Gneiss Belt, southwestern Grenville Province, Canada: a new interpretation.  
451 Canadian Journal of Earth Sciences 37, 217-234.

- 452 Krogh, T. E., Culshaw, N., and Ketchum, J. 1992. Multiple ages of metamorphism and  
453 deformation in the Parry Sound — Pointe au Baril area. Lithoprobe (Abitibi-Grenville  
454 Workshop IV) Report 33, p. 39.
- 455 Lumbers, S.B. 1982, Summary of metallogeny, Renfrew County area: Ontario Geological  
456 Survey Report 212, 58 p.
- 457 Lumbers, S.B and Vertolli, V.M. 2003 Precambrian geology, Kawagama Lake area. Ontario  
458 Geological Survey. Preliminary map P.3525, scale 1:50 000.
- 459 Martin, C. and Dickin, A. P. 2005. Styles of Proterozoic crustal growth on the southeast margin  
460 of Laurentia: evidence from the central Grenville Province northwest of Lac St.-Jean,  
461 Quebec. Canadian Journal of Earth Sciences 42, 1643-1652.
- 462 McNutt, R. H. and Dickin, A. P. 2012. A comparison of Nd model ages and U–Pb zircon ages of  
463 Grenville granitoids: constraints on the evolution of the Laurentian margin from 1.5 to  
464 1.0 Ga. Terra Nova, 24, 7-15.
- 465 Moore, E.S. and Dickin, A.P. 2011. Evaluation of Nd isotope data for the Grenville Province of  
466 the Laurentian Shield using a Geographic Information System (GIS). Geosphere 7, 415-  
467 428.
- 468 Nadeau, L. 1991. Tectonic evolution of the Central Grenville Belt, Huntsville area, Ontario.  
469 Friends of the Grenville Annual Field Excursion, Guidebook.
- 470 Nadeau, L. and van Breemen, O. 1998. Plutonic ages and tectonic setting of the Algonquin and  
471 Muskoka allochthons, Central Gneiss Belt, Grenville Province, Ontario. Canadian  
472 Journal of Earth Sciences 35, 1423-1438.

- 473 Rivers, T., Ketchum, J., Indares, A. and Hynes, A. 2002. The High Pressure belt in the Grenville  
474 Province: architecture, timing, and exhumation. *Canadian Journal of Earth Sciences* 39,  
475 867-893.
- 476 Rivers, T., Martignole, J., Gower, C.F. and Davidson, A. 1989. New tectonic divisions of the  
477 Grenville Province, southeastern Canadian Shield. *Tectonics* 8, 63-84.
- 478 Rivers, T. and Schwerdtner, W. 2015. Post-peak Evolution of the Muskoka Domain, Western  
479 Grenville Province: Ductile Detachment Zone in a Crustal-scale Metamorphic Core  
480 Complex. *Geoscience Canada* 42, 403-436.
- 481 Slagstad, T., Culshaw, N.G., Daly, J.S. and Jamieson, R.A. 2009. Western Grenville Province  
482 holds key to midcontinental Granite-Rhyolite Province enigma. *Terra Nova* 21, 181-187.
- 483 Slagstad, T., Culshaw, N.G., Jamieson, R.A. and Ketchum, J.W. 2004. Early Mesoproterozoic  
484 tectonic history of the southwestern Grenville Province, Ontario: constraints from  
485 geochemistry and geochronology of high-grade gneisses. *Geological Society of America*  
486 *Memoirs* 197, 209-241.
- 487 White, D. J., Easton, R. M., Culshaw, N. G., Milkereit, B., Forsyth, D. A., Carr, S. and  
488 Davidson, A. 1994. Seismic images of the Grenville Orogen in Ontario. *Canadian Journal*  
489 *of Earth Sciences* 31, 293-307.

491 **Table caption**

492 Table 1. Nd isotope data for analysed samples from the Algonquin Park region

493

494 **Table 1 footnote**

495 Petrology key: TN = Tonalite, GD = granodiorite, MG = monzogranite, GR = granite, QD =  
496 quartz diorite, QMD = quartz monzodiorite, DI = diorite, MD = monzodiorite.

497

498 **Figure captions**

499 Fig. 1. Map of the SW Grenville Province showing the location of Algonquin Park (AP) relative  
500 to the structural belts proposed by Rivers et al. (1989): APB = Allochthonous Polycyclic Belt;  
501 NB = North Bay; PS = Parry Sound. Major thrusts: ABT = Allochthon Boundary Thrust; MBB =  
502 Monocyclic Belt Boundary.

503

504 Fig. 2. Lithotectonic domains of the Parry Sound region and the Algonquin region after  
505 Davidson et al. (1982) and Culshaw et al. (1983). Solid and dotted black lines = primary and  
506 secondary shear zones from those papers. Dashed violet line and dotted orange line = alternative  
507 trajectories of the Muskoka sole thrust from Rivers and Schwerdtner (2015) and Culshaw et al.  
508 (2016). Green dashed line = ABT of Ketchum and Davidson (2000). Stars = coronitic olivine  
509 metagabbro (Ketchum and Davidson, 2000).

510

511 Fig. 3. Tectonic map and cross-section of the SW Grenville Province showing terranes  
512 categorized by average TDM age: (pink = 2.7 Ga; yellow = 1.9 Ga; mauve = 1.7 Ga; green =

513 1.55 Ga). LW = Lac Watson; NB = North Bay. Red stars = eclogite; red dots = seismic lines.

514 Solid blue line = line of cross-section.

515

516 Fig. 4. Tectonic map of the Algonquin Park area showing sample localities numbered as in Table

517 1 and categorized by TDM model age. Muskoka domain boundary as follows: dashed blue line =

518 Culshaw et al. (1983); solid black = Lumbers and Vertolli (2003); dotted violet = Rivers and

519 Schwerdtner (2015); dotted orange = Culshaw et al. (2016).

520

521 Fig. 5. Sm—Nd isochron diagram for samples in Table 1 compared with published age suites:

522 Barilia Parautochthon (Dickin et al., 2008); Slagstad et al. (2009) excluding sample E; Muskoka

523 (samples 1-15 from Dickin et al., 2010; samples 60-65 from Dickin et al. 2017).

524

525 Fig. 6. Plot of Epsilon Nd at 1.5 Ga as a function of Nd content for new and published data

526 (symbols as in Fig. 5).

527

528 Fig. 7. Map of central Algonquin Park, showing boundaries in Fig. 4 against a background of the

529 first vertical derivative of the total magnetic field draped over a shaded DEM map. Dashed blue

530 line = Culshaw et al. (1983); solid violet = Rivers and Schwerdtner (2015); dotted orange line =

531 Culshaw et al. (2016); dashed black line = ABT proposed here.

532

533 Fig. 8. View of the north side of the road-cut along Lake of Two Rivers, showing the location of

534 the ABT between a sample of the allochthon (right) and duplex (left) that are ca. 35 m apart.

535 Tom Nagy (pictured) is 1.85 m tall.

Map#	Sample	UTM N NAD 83	UTM E zone 17	Nd ppm	Sm ppm	147Sm/ 144Nd	143Nd/ 144Nd	TDM Ga	E Nd 1.5 Ga	Rock type
Allochthon										
1	KA10	5012860	673070	43.9	9.74	0.1342	0.512186	1.64	3.1	QMD
2	KA24	5020210	679887	10.8	1.93	0.1078	0.511969	1.54	4.0	GD
3	BA28	5050750	697700	24.0	5.86	0.1251	0.512119	1.59	3.6	QD
4	AL57	5050200	698915	31.6	5.78	0.1104	0.511982	1.56	3.7	GD
5	AL40	5051294	704295	20.0	4.00	0.1211	0.512058	1.62	3.1	MD
6	AL21	5058910	704740	30.0	6.06	0.1219	0.512062	1.63	3.1	QMD
7	BA23	5052200	707200	46.2	8.06	0.1054	0.512024	1.43	5.5	DI
8	BA22	5050500	710900	55.8	11.27	0.1221	0.512094	1.58	3.7	DI
9	BA20	5042700	714800	26.2	5.19	0.1197	0.512051	1.61	3.3	MD
10	BA18	5040100	719600	40.5	8.56	0.1278	0.512160	1.56	3.9	MD
11	BA17	5038200	719550	32.4	5.92	0.1103	0.511932	1.64	2.8	GD
12	BA71	5042448	722029	49.6	9.59	0.1167	0.512125	1.44	5.3	MG
13	BA78	5040290	728444	33.9	6.39	0.1140	0.512085	1.46	5.0	QD
14	BA73	5030266	721936	67.7	11.27	0.1007	0.511877	1.56	3.5	GD
15	WH6	5019940	731071	21.1	4.65	0.1332	0.512253	1.49	4.6	QD
							Mean	1.56	3.9	
Duplex										
16	DW23	5017027	659701	35.2	6.84	0.1172	0.511960	1.71	2.0	MG
17	DW24	5021112	659163	41.1	8.16	0.1198	0.511963	1.75	1.5	GD
18	KA6	5013590	666410	77.8	15.89	0.1234	0.512013	1.74	1.8	MG
19	KA1	5016540	666740	80.8	17.08	0.1277	0.512065	1.73	2.0	QSY
20	KA3	5022450	669040	32.9	5.67	0.1042	0.511782	1.75	1.0	MG
21	KA5	5023990	673960	23.2	5.03	0.1309	0.512090	1.75	1.9	QMD
22	KA20	5024200	679700	36.4	5.76	0.0955	0.511697	1.73	1.0	MG
23	DW25	5030510	666796	40.5	5.79	0.0862	0.511650	1.66	1.9	QMD
24	D9	5031500	678100	45.6	7.94	0.1054	0.511815	1.73	1.4	QMD
25	AL46	5040593	676100	52.2	9.49	0.1099	0.511883	1.70	1.9	MG
26	BA25	5041800	677600	46.0	9.49	0.1248	0.512004	1.78	1.4	DI
27	AL45	5044100	679050	65.2	12.77	0.1183	0.511922	1.79	1.0	GR
28	BA26	5045950	681000	37.0	5.86	0.0957	0.511708	1.72	1.2	MG
29	AL60	5043120	680507	42.1	6.11	0.0877	0.511662	1.67	1.8	GR
30	AL61	5042154	681922	31.7	5.09	0.0971	0.511737	1.70	1.5	MG
31	AL32	5048450	689640	25.9	4.90	0.1145	0.511926	1.71	1.8	GD
	AL32R			23.8	4.52	0.1147	0.511922	1.72	1.7	
32	AL31	5049450	692650	57.1	11.06	0.1170	0.511930	1.75	1.4	MG
33	AL30	5050990	695760	41.4	8.28	0.1208	0.512002	1.70	2.1	MG
34	AL43	5051010	696841	35.5	6.68	0.1139	0.511915	1.72	1.7	MG
35	AL42	5050899	697037	27.2	4.09	0.0908	0.511650	1.73	1.0	MG
36	AL20	5062140	704210	50.0	10.57	0.1277	0.512066	1.73	2.0	QD
37	AL27	5064730	704540	25.6	4.43	0.1046	0.511804	1.73	1.3	MG
38	BA48	5050800	726500	50.7	10.25	0.1222	0.512004	1.73	1.9	MG
39	BA70	5045014	733793	63.3	12.39	0.1184	0.511954	1.74	1.6	QD
40	AL47	5039200	683624	59.8	12.55	0.1269	0.512033	1.77	1.5	DI
41	AL34	5047150	685990	30.8	5.97	0.1171	0.511899	1.80	0.8	MG
	AL34R			32.0	6.18	0.1166	0.511906	1.78	1.0	
42	CL5N	5091930	695880	75.8	15.97	0.1274	0.512035	1.78	1.5	GD
43	AQ33	5091200	697600	120.3	23.15	0.1164	0.511933	1.73	1.6	MG
							Mean	1.73	1.5	
Cache Lake										
44	AL33	5047200	686750	85.3	12.18	0.0868	0.511547	1.80	-0.3	MG
45	BA27	5047600	688200	31.5	6.55	0.1259	0.511969	1.86	0.5	QD
46	CL4	5048130	689110	60.5	10.67	0.1065	0.511771	1.81	0.3	GD
47	CL1	5044954	688470	29.9	5.72	0.1155	0.511837	1.87	-0.1	MG

## Oxtongue Lake

48	KA11	5016994	662152	43.7	8.70	0.1201	0.511847	1.95	-0.8	GD
49	DW20	5024707	662006	36.4	6.73	0.1118	0.511827	1.81	0.4	GD
50	DW26	5027248	663040	36.0	8.13	0.1365	0.512088	1.88	0.8	GD

## Heron Lake

51	AL49	5036508	672009	23.0	5.29	0.1390	0.512070	1.98	-0.1	MD
52	AL48	5038800	674614	28.2	6.03	0.1292	0.511986	1.90	0.2	DI
							Mean	1.87	0.1	

## Boundary zone

	AL51	5050816	697535	42.1	8.05	0.1155	0.511921	1.74	1.5	QMD
	AL53	5050797	697575	33.4	5.47	0.0988	0.511820	1.62	2.8	GD

Draft

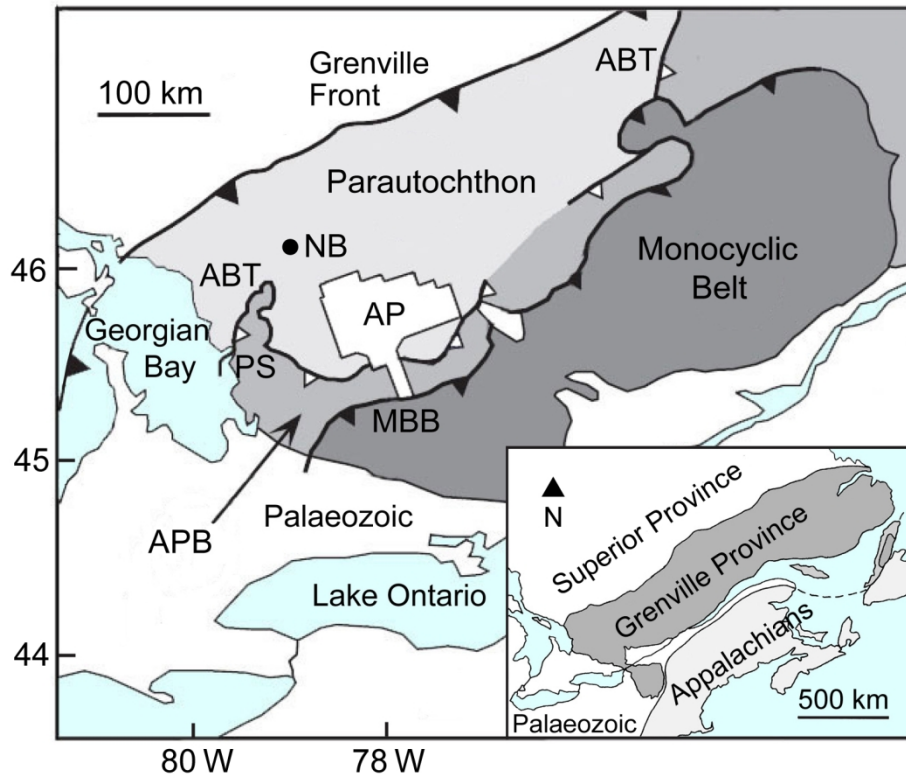


Fig1

152x123mm (300 x 300 DPI)

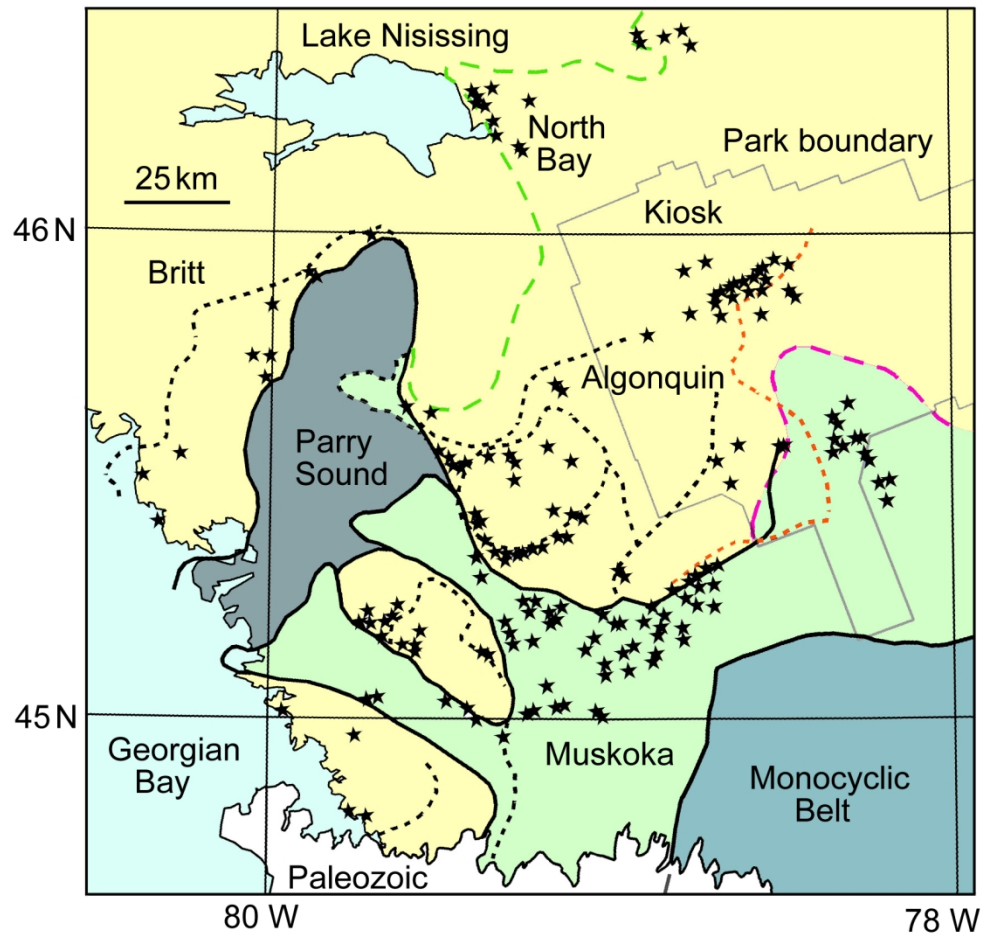


Fig2

152x147mm (300 x 300 DPI)

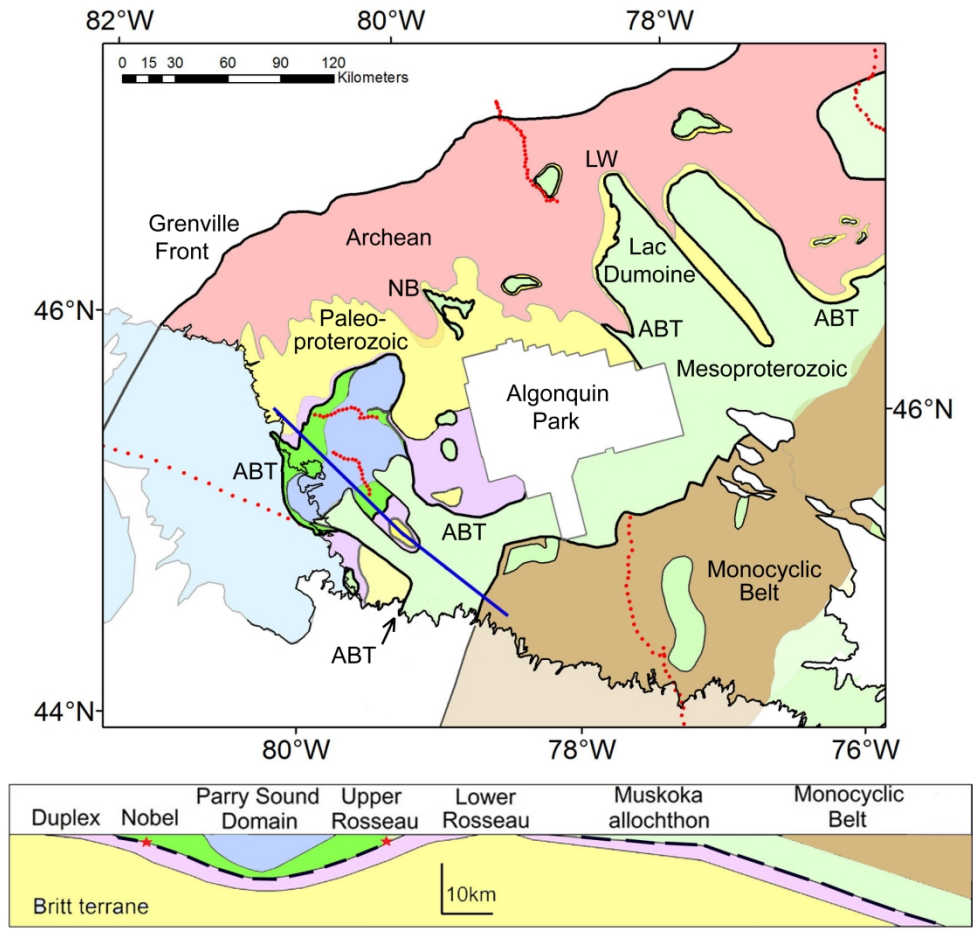


Fig 3

228x220mm (300 x 300 DPI)

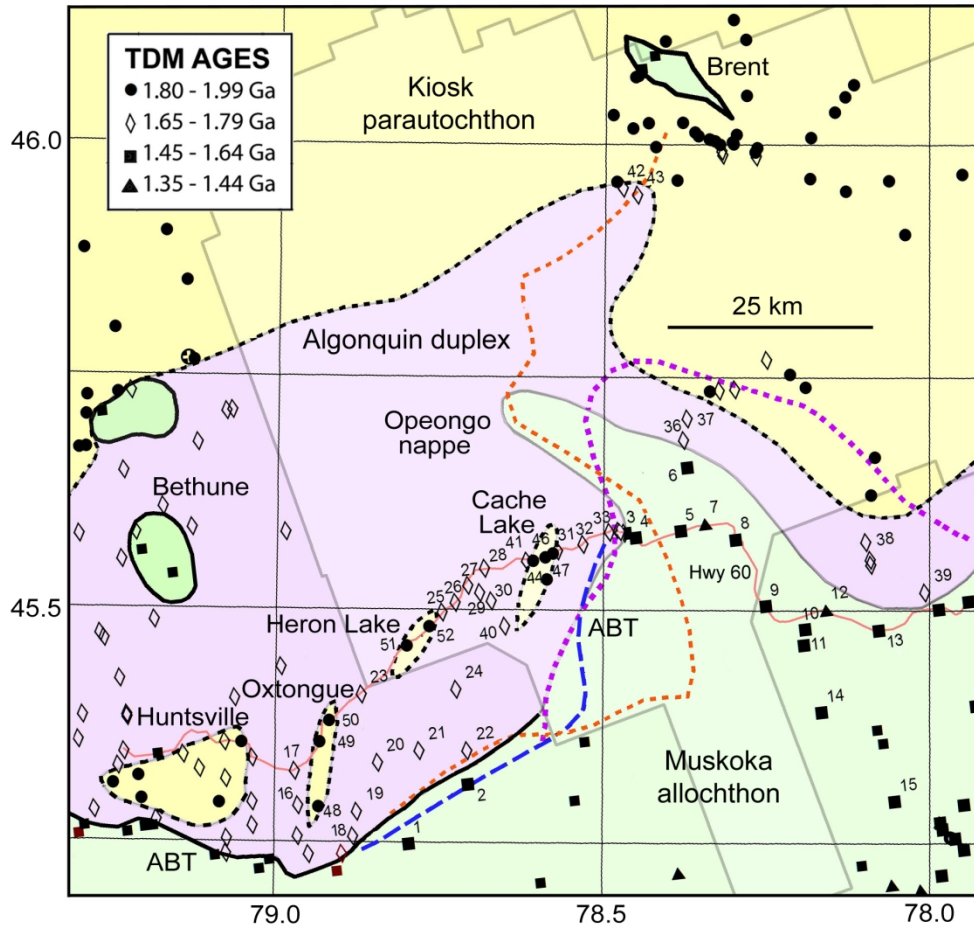


Fig4

168x165mm (300 x 300 DPI)

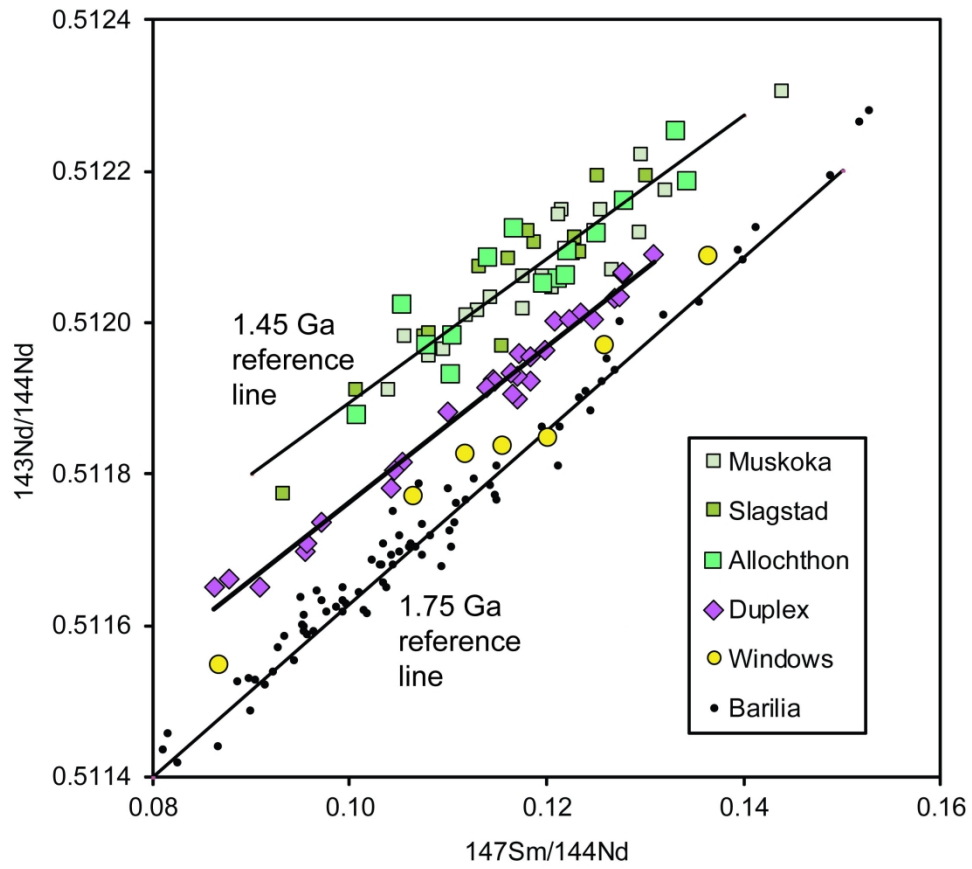


Fig5

217x203mm (300 x 300 DPI)

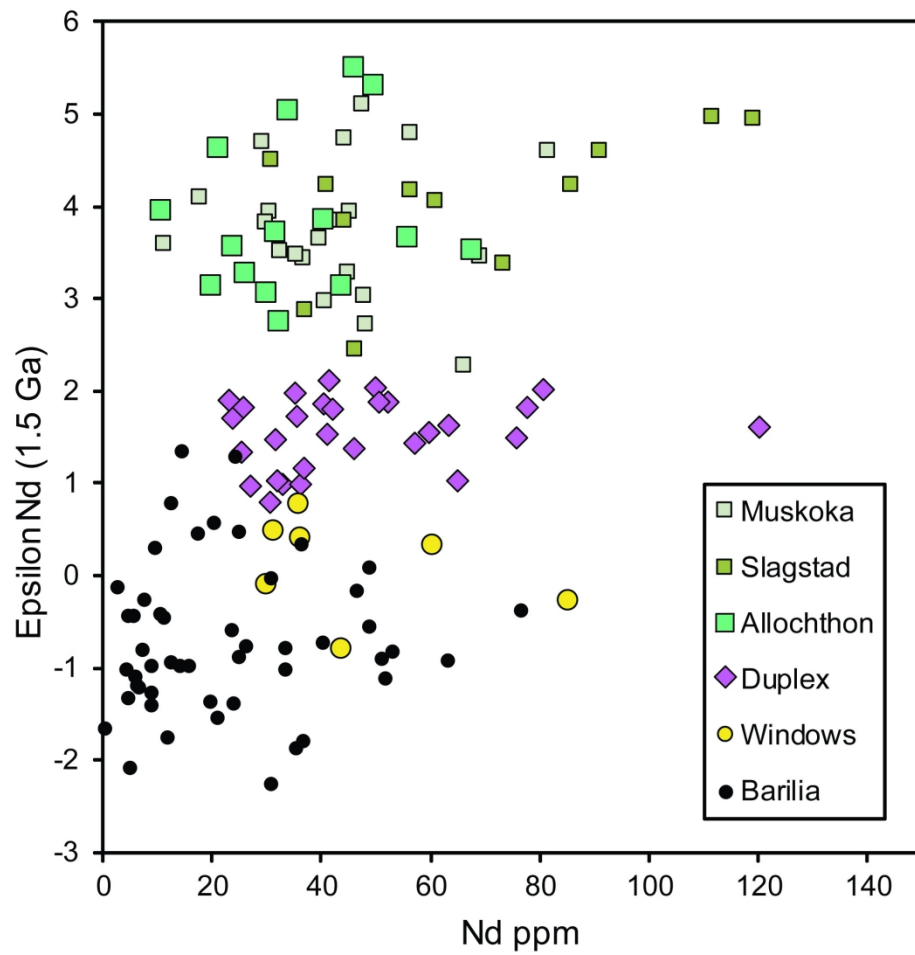


Fig6

197x203mm (300 x 300 DPI)

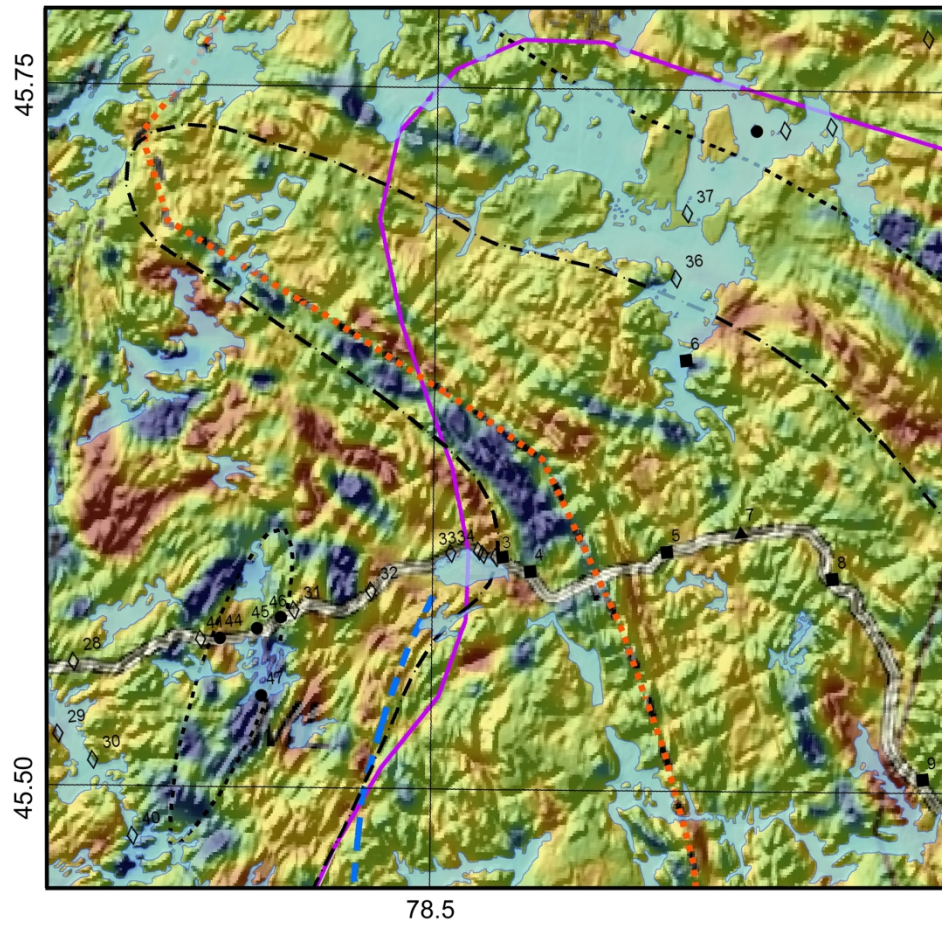


Fig7

167x165mm (300 x 300 DPI)

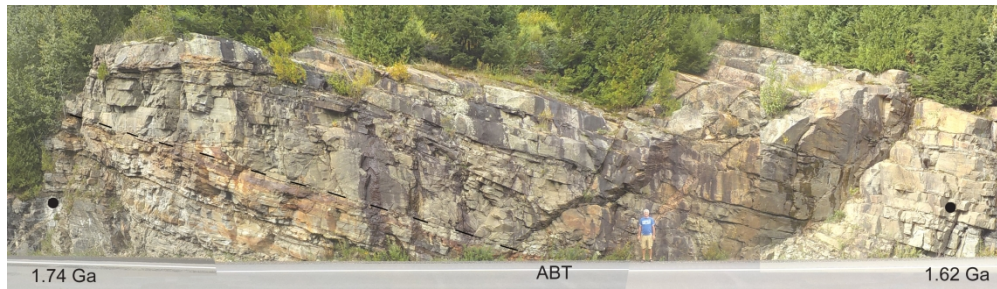


Fig8

266x76mm (300 x 300 DPI)